MECHANICAL VIBRATIONS

MATLAB TEAMWORK PROJECT

A.A. 2023/2024

V6 90° ENGINE VIBRATION ANALYSIS AND DISCUSSION

Group n. 3

GROUP MEMBERS AND ROLES

- Chairman: Filippo Tullio
- Coordinator: Amedeo Moriconi
- Technical tasks
  - Data Research
    - Antonio Maria Macripò
  - CAD Model
    - Michele Palomba
    - Amedeo Moriconi
  - Theoretical developments
    - Michele Chiomento
    - Attilio Marasco
    - Amedeo Moriconi
  - Numerical Implementation
    - Gianmarco Senzamici
    - Michele Palomba
    - Antonio Maria Macripò
  - Graphics
    - Filippo Tullio
    - Attilio Marasco
    - Michele Chiomento
  - FEM and Multibody dynamics Modal Analysis
    - Amedeo Moriconi

INTRODUCTION

The primary aim of the project is to investigate the vibrations generated by the imbalance in a V6-90° internal combustion engine, typical of nowadays Formula 1 competition cars.

The utilization of a Multi-degree of Freedom (N-DOF) model enables a more precise description of physical problems, through the application of techniques that facilitate the conversion of an initial problem, defined by partial differential equations (PDEs) with infinite degrees of freedom. This transformation is accomplished by employing methodologies that yield a system characterized by a specific number of coupled ordinary differential equations (ODEs). These ODEs collectively serve as an approximation of the original PDEs, thus enhancing the accuracy of the system's representation and analysis.

FIGURE 1: REPRESENTATION OF ENGINE AS A RIGID BODY, 3 DAMPERS AND 3 SPRINGS ON EACH OF THE FOUR MOUNTS

As a simplification, the engine block is considered as a rigid body supported by four mounts, through which the vibration forces originating from the engine are transmitted to the chassis. Each mount consists of three springs and three linear dampers, as illustrated, capable of bearing loads only in the main direction (axial). A reference system positioned in the center of mass with axes aligned as in Figure 1 is chosen. The system thus exhibits 6 degrees of freedom: 3 translations along the principal axes x, y and z and 3 rotations around x (roll), y (pitch) and z (yaw) respectively. In analyzing the behavior of the engine block, various stiffness and damping coefficients for each mount, as provided by the manufacturer [1], are taken into consideration.
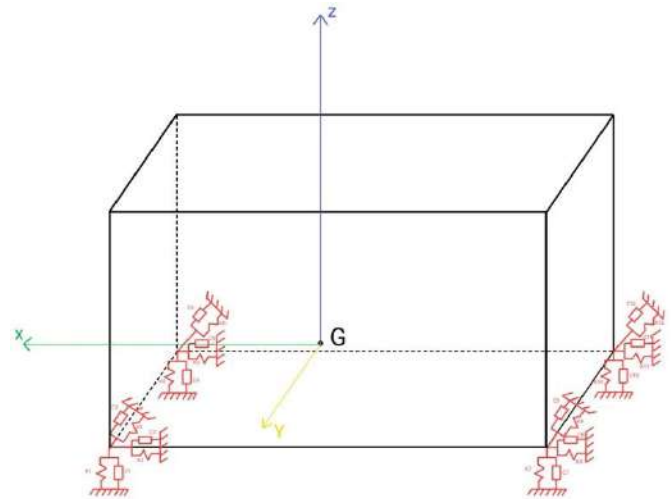
A V6 engine with a 90-degree angle between the cylinder banks provides several advantages, including compactness, balance, and reduced vibrations during operation.

Although this configuration stands out for its application in the Formula 1 realm, owing to the limited availability of accessible data, the group based its research and considerations drawing inspiration from the "Nettuno" engine by Maserati, introduced in 2020 and featured in the cutting-edge MC20.

The aims delineated in the ensuing report encompass the formulation of a dynamic model to investigate V6-90° vibrations, identification of inertial forces resulting from reciprocating component motion, derivation of the system's equation of motion, exploration of natural frequencies and mode shapes, execution of ramp tests and steady-state ramp analysis. Subsequently, the ultimate goal of the project involves plotting and examining in detail the displacements and accelerations of the center of mass, along with the forces transmitted to the chassis, as functions of both time and frequency across three distinct operational regimes of interest. The regimes of 2000rpm, 3000rpm, and 7500rpm have been selected: the first corresponds to the maximum highway cruising speed (130km/h) in the highest

FIGURE 2: CAD MODEL

gear, the second and third are chosen as they ensure the maximum torque (730Nm) and power (630hp) that can be utilized by the engine, respectively.
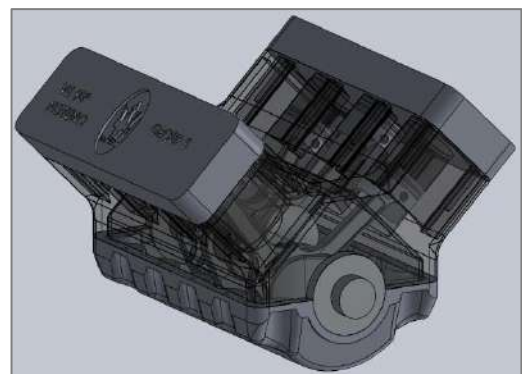
The data found in literature is employed to build a reliable CAD model on SOLIDWORKS, including the crankshaft. Thereafter, leveraging the "*Evaluate mass properties*" function within the software, we successfully acquired the inertia matrix of the engine block and the precise position of the center of mass. [2]

THEORY

The theoretical development begins with the search for the motion equation using the Lagrange's equations energetic approach, considering separately the terms of kinetic energy (T), potential energy (U), and Rayleigh's dissipation function (D):

$$\frac{d}{dt}\left(\frac{\partial T}{\partial \dot{q}_i}\right) + \frac{\partial U}{\partial q_i} + \frac{\partial D}{\partial \dot{q}_i} = Q_i \tag{1}$$

Where the counter 'i' ranges from 1 to n based on the number of degrees of freedom (in this case, six). The system is initially considered damped, and the three coordinates of the COG, together with the three rotations around the principal axes, are chosen as the basic Lagrangian coordinates: $q_1 = x_G$, $q_2 = y_G$, $q_3 = z_G$, $q_4 = \theta_x$, $q_5 = \theta_y$, $q_6 = \theta_z$. Q_i represent the forcing vector i^{th} component, which will be calculated later on.

Upon developing the motion equation, the following displacements Δ_i of the mounts positioned in A, B, C, and D are obtained as functions of the previous coordinates, considering the dimensions of the body.
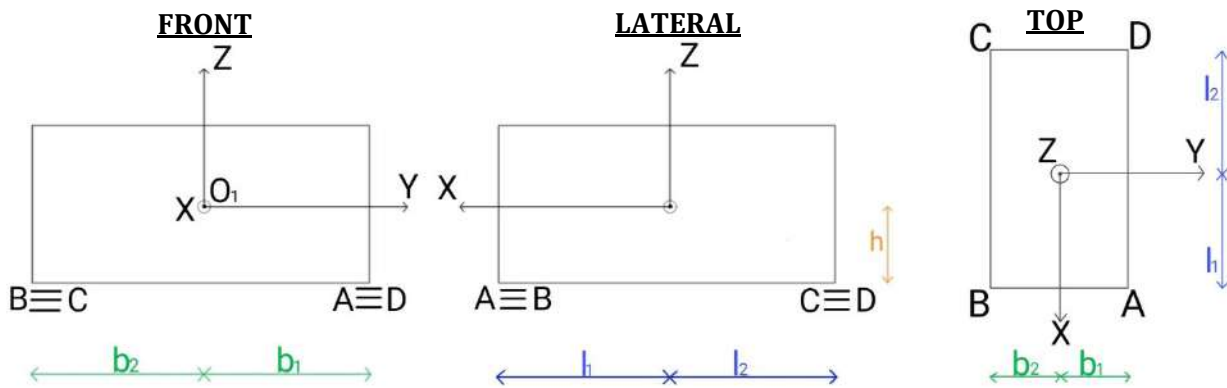

FIGURE 3: VIEWS OF THE SIMPLIFIED ENGINE BLOCK

$$\Delta_A = \begin{bmatrix} \Delta_{xA} \\ \Delta_{yA} \\ \Delta_{zA} \end{bmatrix} = \begin{bmatrix} x - \theta_z b_1 - \theta_y h \\ y + \theta_z l_1 + \theta_x h \\ z - \theta_y l_1 + \theta_x b_1 \end{bmatrix} \quad \Delta_B = \begin{bmatrix} \Delta_{xB} \\ \Delta_{yB} \\ \Delta_{zB} \end{bmatrix} = \begin{bmatrix} x + \theta_z b_2 - \theta_y h \\ y + \theta_z l_1 + \theta_x h \\ z - \theta_y l_1 - \theta_x b_2 \end{bmatrix}$$

$$\Delta_C = \begin{bmatrix} \Delta_{xC} \\ \Delta_{yC} \\ \Delta_{zC} \end{bmatrix} = \begin{bmatrix} x - \theta_y h + \theta_z b_2 \\ y + \theta_x h - \theta_z l_2 \\ z - \theta_x b_2 + \theta_y l_2 \end{bmatrix} \quad \Delta_D = \begin{bmatrix} \Delta_{xD} \\ \Delta_{yD} \\ \Delta_{zD} \end{bmatrix} = \begin{bmatrix} x - \theta_y h - \theta_z b_1 \\ y + \theta_x h - \theta_z l_2 \\ z + \theta_x b_1 + \theta_y l_2 \end{bmatrix} \tag{2}$$

At this point, initially neglecting the force analysis, presented later, the kinetic energy T is calculated under the assumption of small translations and rotations as follows:

$$T = \frac{1}{2} m\left(\dot{x}_G^2 + \dot{y}_G^2 + \dot{z}_G^2\right) + \frac{1}{2}\left[J_{xx}\dot{\theta}_x^2 + J_{yy}\dot{\theta}_y^2 + J_{zz}\dot{\theta}_z^2 + 2J_{xy}\dot{\theta}_x\dot{\theta}_y + 2J_{xz}\dot{\theta}_x\dot{\theta}_z + 2J_{yz}\dot{\theta}_y\dot{\theta}_z\right] \tag{3}$$

The second term considered is the potential energy, calculated by summing up its respective components in the three principal directions:

$$U = U_x + U_y + U_z = \frac{1}{2}k_x(\Delta_{xA}^2 + \Delta_{xB}^2 + \Delta_{xC}^2 + \Delta_{xD}^2) + \frac{1}{2}k_y(\Delta_{yA}^2 + \Delta_{yB}^2 +$$

$$\Delta_{yC}^2 + \Delta_{yD}^2) + \frac{1}{2}k_z(\Delta_{zA}^2 + \Delta_{zB}^2 + \Delta_{zC}^2 + \Delta_{zD}^2) \tag{4}$$

For simplicity, the stiffness of the four supports has been considered of equal value along the same axes. Finally, the last term considered is the dissipation function (Rayleigh), subsequently employed to determine the damping matrix:

$$D = \sum_{i=x}^{z} \sum_{p=A}^{D} \frac{1}{2} C_i \dot{\Delta}_{ip}^2 = D_x + D_y + D_z = \frac{1}{2}C_x \sum_{p=A}^{D} \dot{\Delta}_{xp}^2 + \frac{1}{2}C_y \sum_{p=A}^{D} \dot{\Delta}_{yp}^2 + \frac{1}{2}C_z \sum_{p=A}^{D} \dot{\Delta}_{zp}^2 \tag{5}$$

The equation (1) can subsequently be reformulated in matrix form:

$$M\ddot{q} + C\dot{q} + Kq = Q \tag{6}$$

Where the matrix **M** is the mass matrix, being directly associated with the expression of kinetic energy, which remains consistently positive, is symmetric and *positive-definite*. **C** is known as the damping matrix and is symmetric too. Conversely, the matrix **K** is known as the stiffness matrix that is both symmetric according to Betti's reciprocity theorem and *positive semi-definite* as it is associated with the potential energy of the rigid body, which can be positive or, at most, zero.

$$M = \begin{bmatrix} m & 0 & 0 & 0 & 0 & 0 \\ 0 & m & 0 & 0 & 0 & 0 \\ 0 & 0 & m & 0 & 0 & 0 \\ 0 & 0 & 0 & J_{xx} & J_{xy} & J_{xz} \\ 0 & 0 & 0 & J_{yx} & J_{yy} & J_{yz} \\ 0 & 0 & 0 & J_{zx} & J_{zy} & J_{zz} \end{bmatrix} \tag{7}$$

$$K = \begin{bmatrix} 4k_x & 0 & 0 & 0 & -4k_xh & 2k_x(b_2 - b_1) \\ 0 & 4k_y & 0 & 4k_yh & 0 & 2k_y(l_1 - l_2) \\ 0 & 0 & 4k_z & 2k_z(b_1 - b_2) & 2k_z(l_2 - l_1) & 0 \\ 0 & 4k_yh & 2k_z(b_1 - b_2) & 4k_yh^2 + 2k_z(b_1^2 + b_2^2) & k_z(-l_1b_1 + l_1b_2 + l_2b_1 - l_2b_2) & 2k_xh(b_1 - b_2) \\ -4k_xh & 0 & 2k_z(l_2 - l_1) & k_z(-l_1b_1 + l_1b_2 + l_2b_1 - l_2b_2) & 4k_xh^2 + 2k_z(l_1^2 + l_2^2) & 2k_xh(b_1 - b_2) \\ 2k_x(b_2 - b_1) & 2k_y(l_1 - l_2) & 0 & 2k_yh(l_1 - l_2) & 2k_xh(b_1 - b_2) & 2k_x(b_1^2 + b_2^2) + 2k_y(l_1^2 + l_2^2) \end{bmatrix} \tag{8}$$

However, due to the lack of data regarding the coefficients of **C**, a more common approach in engineering practice, known as proportional damping, is adopted instead of considering the dissipation function. In this method, by setting a target value for the damping ratios 'ζ_i', the parameters α and β are adjusted to distribute damping across both low and high frequencies and **C** matrix is then obtained:

$$\zeta_i = \frac{1}{2}\left(\frac{\alpha}{\omega_{r_i}} + \beta\omega_{r_i}\right), \quad i = 1, \dots, n \tag{9}$$

$$C = \alpha M + \beta K \tag{10}$$

At this stage, natural frequencies and modal shapes can be computed by solving a non-standard eigenvalue problem considering the undamped system, as shown:

$$det(K - \omega^2 M) = 0 \tag{11}$$

Where the ω_i^2 (i=1, …, n) in the equation are the eigenvalues of the matrix and represent the square of the system's natural frequencies, while each vibrational mode shape is obtained through the eigenvector u_i associated to each eigenvalue, given by: [3]

$$(K - \omega_i^2 M)u_i = 0 \tag{12}$$

Let's now calculate the forces to complete the right-hand side of the Lagrange's equation. First of all, as a simplification, forces and torques deriving from the combustion phase are not considered because they are essential for generating the driving torque. Additionally, these forces are internal to the system and have a net result of zero (they indeed only produce a pure torque, which is the driving torque).

The force analysis begins with the displacement (s) of the piston in the simplified system involving a single piston connected to the connecting rod of length (l), which in turn is linked to the crankpin with a radius (r), as illustrated.
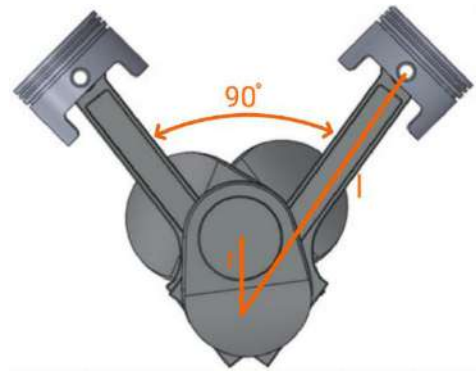

FIGURE 4: THRUST CRANK MECHANISM

$$s_i = r\cos\Theta_i + l\sqrt{1 - \left(\frac{r}{l}\sin\Theta_i\right)^2} \qquad for\ i = 1{:}6 \tag{13}$$

Considering the angular speed (ω) constant, the displacement is differentiated twice with respect to time to obtain the piston's acceleration that, due to the natural balancing of the inertial forces in the V6-90° type engine, is evaluated by means of the Fourier expansion of the acceleration exact form:

$$\ddot{s}_i = -r\omega^2 \left\{ \cos(\omega t + \psi_i) - \frac{r[l^2 - 2l^2\cos^2(\omega t + \psi_i) - r^2\sin^4(\omega t + \psi_i)]}{[l^2 - r^2\sin^2(\omega t + \psi_i)]^{\frac{3}{2}}} \right\} = -r\omega^2 f_i(\theta_i) \qquad for\ i = 1:6 \quad (14)$$

where:

$$f_i(\theta_i) = \frac{a_0}{2} + \sum_{n=1}^{n=4} a_n \cos(n\theta_i) + \sum_{n=1}^{n=4} b_n \sin(n\theta_i) \qquad for\ i = 1:6 \qquad (15)$$

with $\theta_i = \omega t + \psi_i$, where ψ_i is defined as the angle between the rod-journals corresponding to the 1st and the ith cylinder:

$$\boldsymbol{\psi} = \left[0, \frac{2}{3}\pi, \frac{4}{3}\pi, \frac{\pi}{2}, \frac{7}{6}\pi, \frac{11}{6}\pi\right]^T \qquad (16)$$

The coefficients a_n and b_n are computed for each cylinder through a dedicated MATLAB script.

Subsequently, this acceleration expression is employed to determine the inertial forces F_i:

$$F_i = m_B\ddot{s}_i = -m_B r\omega^2 f_i(\theta_i) \qquad for\ i = 1:6 \qquad (17)$$

Where m_b is the translational mass, calculated as the sum of one piston mass and one conrod translating mass. At this point, we project the forces along the y and z axes:

$$F_y = \frac{\sqrt{2}}{2}\left(\sum_{i=4}^6 F_i - \sum_{i=1}^3 F_i\right) \qquad F_z = \frac{\sqrt{2}}{2}\left(\sum_{i=1}^6 F_i\right) \qquad (18)$$
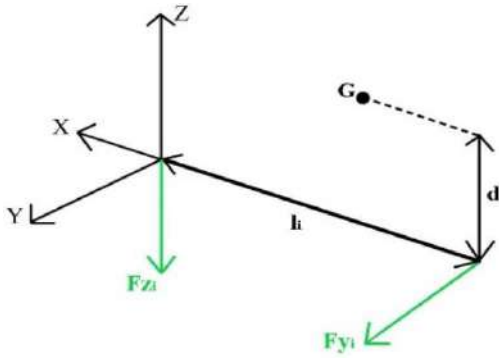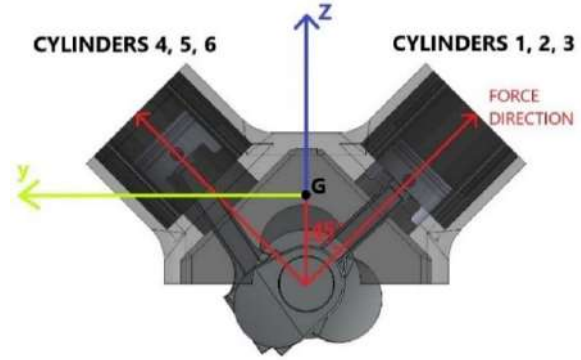

FIGURE 6: FORCES LEVER ARMS

FIGURE 5: REFERENCE SYSTEM

The centrifugal forces are now analyzed: the centrifugal force of a single V2 is considered because two connecting rods are placed in the same rod-journal:

$$F_{Ci} = m_a\omega^2 r(\sin(\omega t + \varphi_i) + \cos(\omega t + \varphi_i)) \qquad for\ i = 1:3 \qquad (19)$$

Where m_a is the rotational mass, defined by the sum of two con-rods and the journal rotational masses, φ_i stands for the phase shift between the three V2s. It's possible to see that the total centrifugal force is given by the sum of three rotating vectors, phase-shifted by 120° and having the same magnitude: this means that the total centrifugal force is always zero.

Now it is possible to calculate the inertia moment acting along the x-axis:

$$M_{in,i} = \frac{1}{2}m_b r^2\omega^2\left[\frac{(-1+\sqrt{3})r}{4l}\sin(\omega t + \psi_i) + \sin(2\omega t + 2\psi_i) - \sqrt{3}\cos(2\omega t + 2\psi_i) - \frac{9r}{2l}\sin(3\omega t + 3\psi_i) + \right.$$
$$\left. + \frac{9r}{2l}\cos(3\omega t + 3\psi_i)\right] \qquad for\ i = 1:6 \qquad (20)$$

It's now possible to define the **Q** vector as follows:

$$\boldsymbol{Q} = [F_x \quad F_y \quad F_z \quad M_x \quad M_y \quad M_z]^T = \left[0 \quad \sum_{i=1}^6 F_{y,i} \quad \sum_{i=1}^6 F_{z,i} \quad \sum_{i=1}^6 M_{in,i} + \sum_{i=1}^6 F_{y,i}\cdot d \quad \sum_{i=1}^6 F_{z,i}\cdot l_i \quad \sum_{i=1}^6 F_{y,i}\cdot l_i\right]^T \qquad (21)$$

6

NUMERICAL IMPLEMENTATION

This section addresses the numerical implementation of the theory discussed in the previous paragraph. The numerical implementation is divided into 3 different scripts: the first computes the forcing calculation, the second one regards the steady state condition and the last one analyzes the ramp test.

FORCING CALCULATION: the first script under analysis is "MV_project_forcing.m", a script which calculates the expression of pistons accelerations by means of the Fourier series expansion. From line **16**, the integration data is defined: the integration interval $[0, 2\pi]$, integral limits and number of harmonics are defined. From line **26** to line **53** the accelerations of the pistons in the first three cylinders, which belong to the right bank of the engine, are computed. Firstly, the angular displacements between the respective crankpins and the expressions of the harmonic components of the piston accelerations, denoted in theory as $f_i(\theta_i)$, are defined. Subsequently, the a_0 coefficient and an initial value to f_x, that represents the Fourier series expansion of $f_i(\theta_i)$, are assigned. Finally, through a **for-end** loop, the coefficients a_n and b_n, along with f_x, are calculated for each cylinder. In the successive lines, the same calculations are performed for the other cylinders.

STEADY STATE RAMP: according to the "MV_project_ss.m" script, engine data and the motion equation matrices **M** and **K** are defined, with a verification of their symmetry using the Cholesky decomposition.

Between lines **44** and **48**, the time interval for the ramp is defined, and subsequently, it is subdivided into 100 time intervals. A vector comprising the 100 corresponding time values (in respect to the ramp test) and their respective angular velocities of interest is subsequently defined.

From line **115** to **149** the proportional damping matrix is defined. Firstly, the damping ratio values are set equal to 0.1 for each DOF. Then, by solving of the Ordinary Least Square problem, the alpha and beta values are obtained. As a solving strategy, the QR numerical solver is implemented.

To solve the motion equation, a modal analysis is performed for decoupling the initial ODEs in time, which are then solved by means of the convolution integral.

MODAL ANALYSIS

From line **102** to line **114**, the eigenvalues and eigenvectors are calculated by means of the **eig** function, which gives as output two 6x6 matrix: the first matrix (**U**) columns are the eigenvectors, while the second one is a diagonal matrix containing the eigenvalues, from which the natural frequency are obtained.

From line **150** to line **171**, the modal analysis is carried on. After the normalization of the eigenvectors matrix, it's possible to take advantage of the orthonormality conditions to verify that **Λ** is a diagonal matrix containing the eigenvalues and **I** is an identity matrix:

$$U^T M U = I \qquad U^T K U = \Lambda \tag{22}$$

In the next section, the problem discretization is performed. Firstly, the time interval is discretized into small time intervals dt=0.0001s and the time vector is subsequently defined, being sure that the Shannon-Nyquist theorem is respected, to avoid the aliasing phenomena: the sampling frequency (reciprocating of dt) must be at least twice the maximum signal frequency.

After this section, some frequency specifications are defined, which will be used for the **fft** computation.

In the "calculation of the displacement" section starting from line **187**, θ is computed for every regime, the forcing matrix is converted to the modal space, then the responses to the unitary impulse are computed for every DOF and for every instant of time by means of a for-end loop cycle. After these calculations, the displacements are calculated by means of the **conv** MATLAB function.

100 REGIMES ANALYSIS

From line **357** to **470** the maximum and root mean square value of the 100 regimes displacements are computed, by means of the **max** and **rms** MATLAB function.

In the next section, the three significant regimes spectrum is evaluated. First of all, the 3-dimensional **q_ss** vector is reduced to a 2D one by means of the **squeeze** MATLAB function, then a **fft** is performed for every DOFs.

Before plotting the spectrum (for simplicity only for the first DOF), a **fftshift** is performed so the zero-frequency component is shifted to array center, so only the positive frequencies are considered.

From line **588** to **683**, the velocities and accelerations of the COG are computed for all the regimes (and plotted for the three significant regimes), by 'squeezing' **q_ss** and using the **gradient** MATLAB function.

In the next section, the forces transmitted to the chassis in all the regimes are computed. For the three regimes of interest, they are also plotted. These forces are defined as:

$$T_{i,p} = c_i \dot{\Delta}_{i,p} + k_i \Delta_{i,p} \qquad i = x, y, z; \quad p = A, B, C, D \qquad (23)$$

RAMP TEST: analyzing the script "MV_project.m", from line **14** to **34** a selector is implemented, to choose whether to analyze the ramp up (from 0 to 8000 rpm) or ramp down (from 8000 to 0rpm).

The engine data, the motion equation, and the time vector are defined in accordance with the steady state ramp script.

To solve the motion equation, two different approaches are adopted:

- Modal analysis, decoupling of ODEs in time domain and solving using the convolution integral.
- Direct numerical integration of the ODEs in time domain.

The modal analysis, the convolutional integral, velocities and accelerations of the center of mass are computed in accordance with the steady state ramp script, with the exception that the **squeeze** function is not required, because all the matrices are two-dimensional.

<u>DIRECT NUMERICAL INTEGRATION</u>: the numerical solver ODE45 admits as input only ordinary differential equation of the first order, so a vector **u** needs to be defined:

$$\boldsymbol{u} = [\boldsymbol{q} \ \dot{\boldsymbol{q}}]^T \qquad (24)$$

By rearranging the equation of motion, a system of two ODEs can be written:

$$\begin{cases} \dfrac{d\boldsymbol{q}}{dt} = \dot{\boldsymbol{q}} \\ \dfrac{d\dot{\boldsymbol{q}}}{dt} = \boldsymbol{M}^{-1}\boldsymbol{C}\dot{\boldsymbol{q}} - \boldsymbol{M}^{-1}\boldsymbol{K}\boldsymbol{q} + \boldsymbol{M}^{-1}\boldsymbol{Q} \end{cases} \qquad (25)$$

By expressing the system in matrix form and applying the **u** vector definition:

$$\dot{\boldsymbol{u}} = \boldsymbol{A}\boldsymbol{u} + \boldsymbol{B} \qquad (26)$$

Within the MATLAB script, the Q components are initially converted from symbolic functions into time-dependent functions using the **matlabFunction** command. Subsequently, matrices A and B are computed. Note that $\boldsymbol{u}$ is a 12-component vector, with the first six components representing the DOFs of the system and the remaining six components representing their derivatives.

At line **507**, the **ode45** solver is employed to compute a solution with homogeneous initial conditions. For the rising ramp test, the system starts from an equilibrium condition with zero initial displacements and velocities, while for the ramp down case, the homogeneous IC are a simplification due to the initial non-zero velocities. This translates in an initial incorrect behavior of the latter, which becomes correct (verified because the trend is mirrored in respect to the rising ramp test result) after the transient finish.

The solver output consists of the time vector and the displacement vector, which are plotted in the following lines.

In the next section, the forces transmitted to the chassis are defined as before and plotted.

Subsequently, from **line 644** the normalized modes (eigenvectors) are plotted.

<u>MODES PLOT</u>: the modes plot, last section of the script, serve the purpose of giving a graphic visualization of the interaction between every mode and its DOFs excitation contribute.

RESULTS

FORCING CALCULATION

The script "forcing_calculation.m" gives as output the matrices of the coefficient a_n and b_n, and the harmonic component of the piston acceleration plot, see figure xx.

As expected, due to the odd firing order of the Nettuno engine, the piston accelerations for a fixed value of the angular speed are shifted by 30° and 90°.
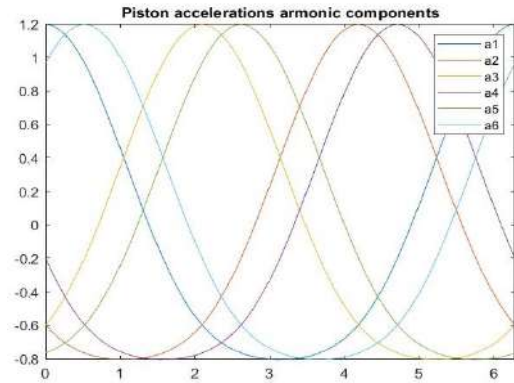

FIGURE 7: ACCELERATIONS TREND

STEADY STATE RAMP: The first result obtained by the steady state ramp script are the coefficient defining the damping matrix:

$$\alpha = 9.1183 \qquad \beta = 0.000894 \tag{27}$$

Subsequently, the script validates the theory development by confirming that the **M** and **K** matrices are symmetric and positive definite.

MODAL ANALYSIS: the most relevant results obtained from the modal analysis section are the eigenvectors, stored as columns of the **modes** matrix and the natural circular frequencies $\omega_{n,i}$:

$$\boldsymbol{\omega_n} = [57.78 \ 61.86 \ 85.28 \ 138.18 \ 159.63 \ 180.98]^T \qquad \left[\frac{rad}{s}\right] \tag{28}$$

MAX AND RMS VALUES: after solving for the displacement vector **q** by means of the convolutional integral, the MAX and RMS values for each of the 100 regimes are plotted. For simplicity, only the first two DOFs are shown here:
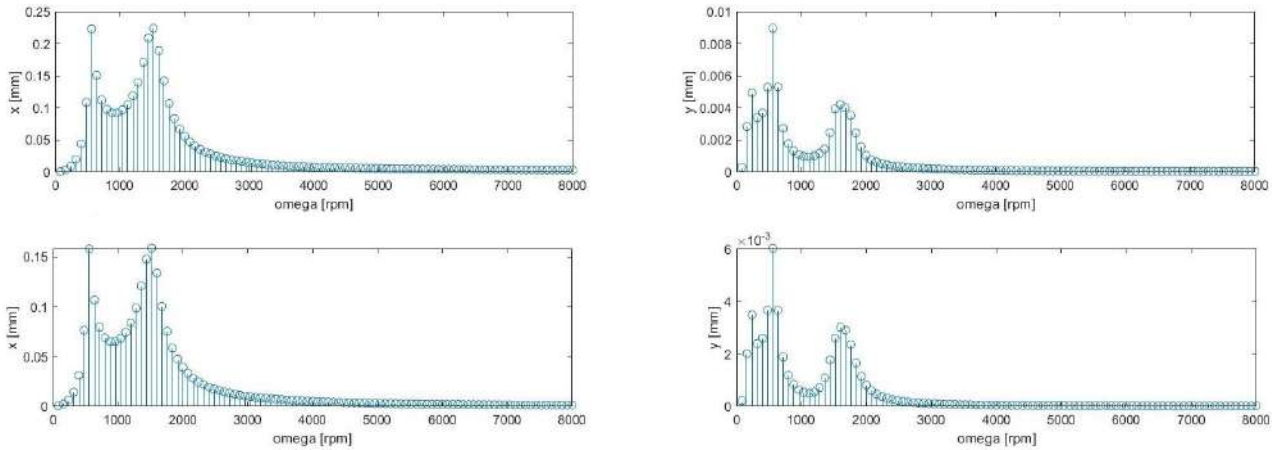

FIGURE 8: MAX (UP) AND RMS (DOWN) VALUE

Near the resonance frequencies, the MAX and RMS value increase rapidly, depending on which frequency and which DOF is considered, because for every mode of the system one or more DOFs are more excited than the others.

SIGNIFICANT REGIMES: The next results are regarding the three regimes of interest: the COG displacement and acceleration are computed and plotted to visualize their trend along time. In figure 10 the displacement and accelerations of the first three DOFs are plotted. The max values are consistent with the ones found before at those regimes. The COG displacements are a linear combination of different periodic functions (whose can be seen in the displacement spectrum) and their amplitude depends on the proximity of the regime considered to a resonance frequency and on the corresponding force and moments magnitude. The most relevant value is recorded along the x direction.
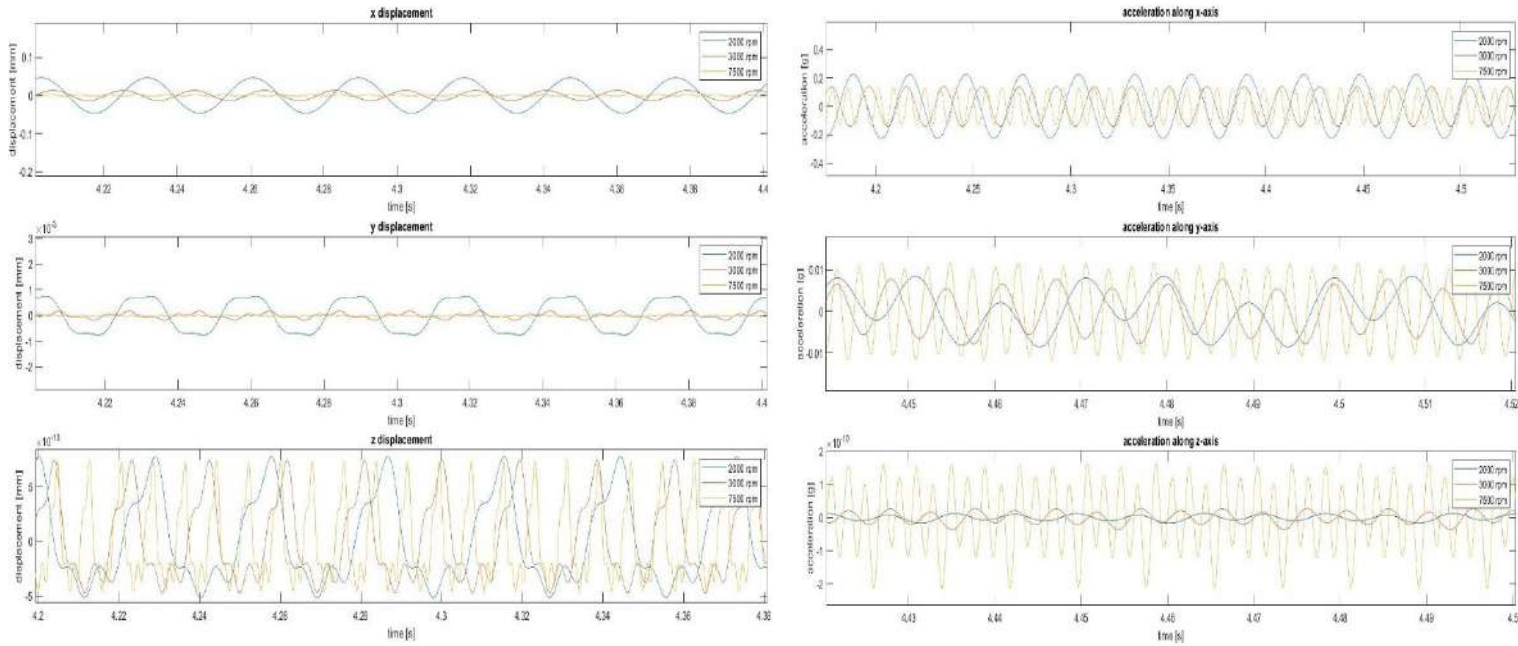
9

FIGURE 9: COG DISPLACEMENT AND ACCELERATIONS

SPECTRAL ANALYSIS: to visualize the harmonic components of the COG displacement, the spectrum of q is plotted (for simplicity only for the first DOF, but it's easy to plot also the other DOFs spectrum) for the 3 significant regimes. The main contributes are found near to the considered regime frequency.
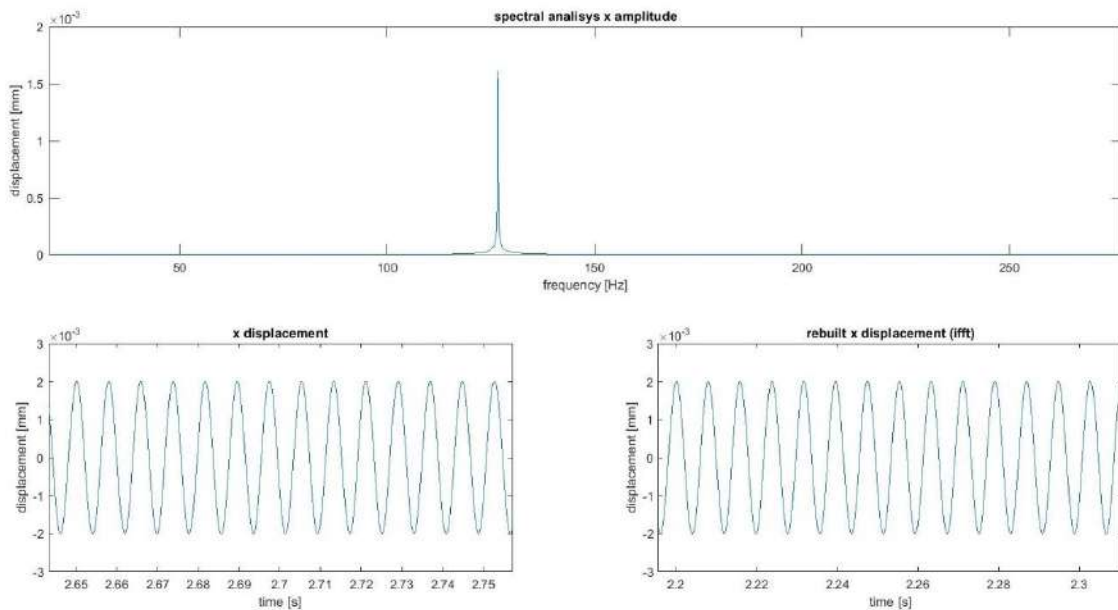

FIGURE 10: SPECTRUM AND DISPLACEMENT FOR 7500 RPM

TRANSMISSIBILITY: The highest value of displacement is along the z direction at 2000 rpm, which is the closest regime to a resonance frequency. From the transmissibility plot, a consistent result is obtained: the highest force value is in the z direction, at 2000 rpm, of about 775N.

RAMP TEST: The results are discussed of the ramp up subcase. The same considerations apply for the ramp down subcase. The first interesting result of the ramp test is the forces trend in time, where the magnitude grows quadratically and it's the same for every cylinder.

After the force plot, the solutions obtained by the convolution integral in the modal space and the direct numerical solution are computed and plotted, see figure 12

10

As expected, every DOFs displacements is characterized by its highest values in correspondence of the natural frequency that has the highest modal participation for that DOF. A similar behavior is found in some accelerations plot.

Due to the increasing rotational speed, the COG displacements frequency increases with time. So, their second derivatives, which are the COG accelerations along the DOFs, grow with time.

To visualize the difference between the two methods, the displacements along the x direction are plotted in the same chart. The results are satisfying, with a slightly error of

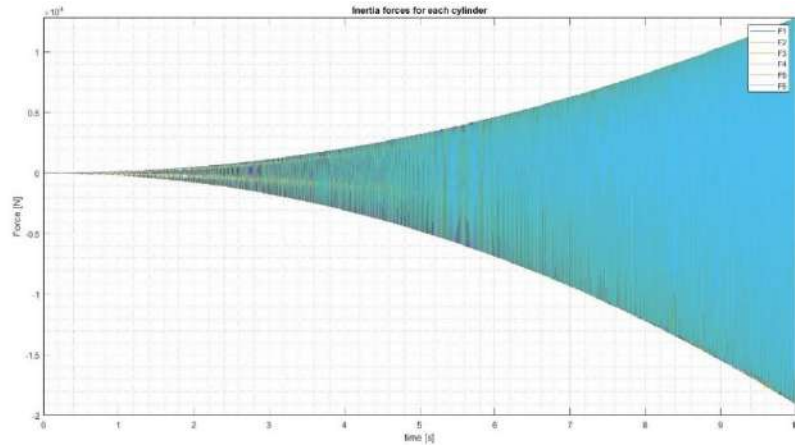FIGURE 11: INERTIAL FORCES TREND

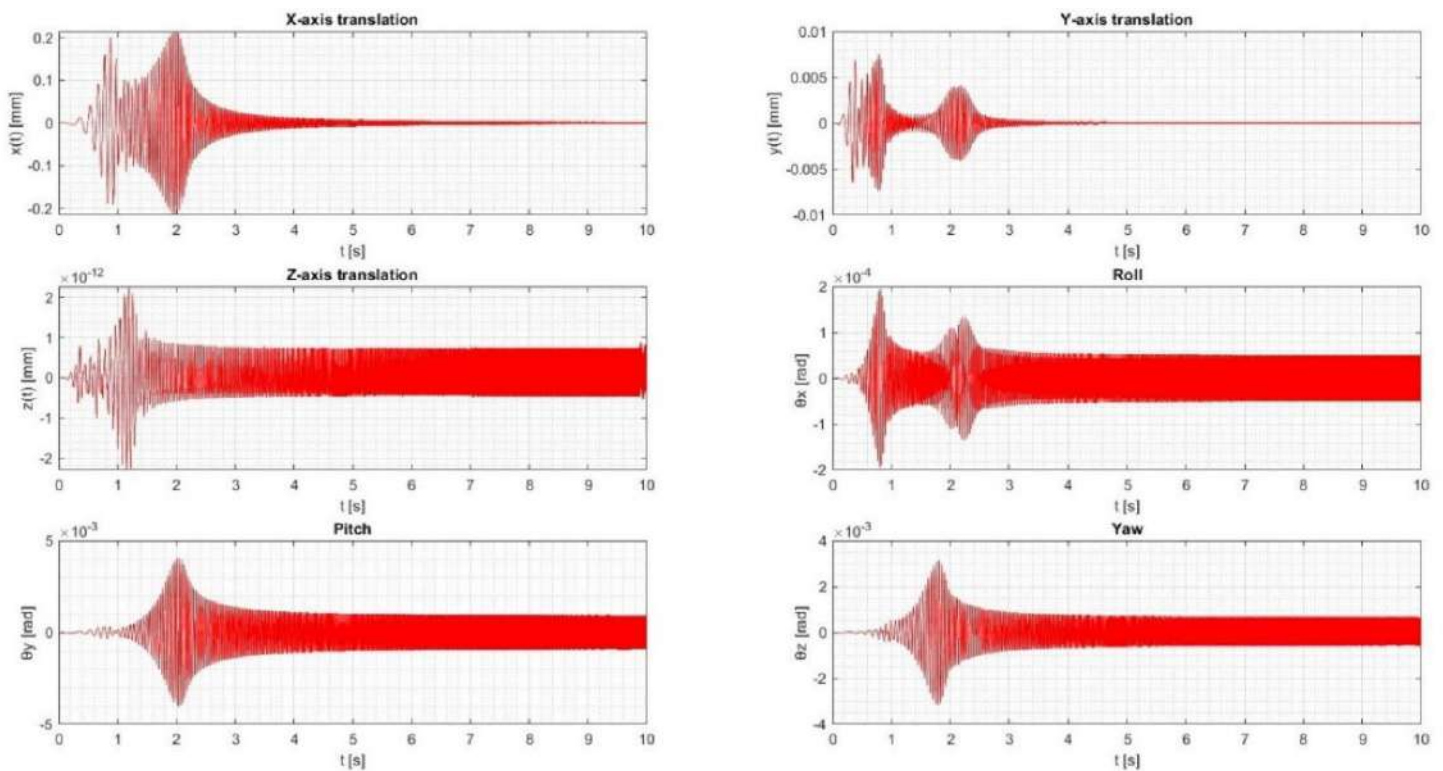value about 0.015mm only in correspondence on the peaks of the signal.

FIGURE 12: ODE45 NUMERICAL SOLUTION

TRANSMISSIBILITY: The transmissibility trend is consistent with the displacement one, with the maximum value of about 2kN in correspondence of the resonance frequency crossed during the ramp. After crossing these critical frequencies, the force magnitude decreases very quickly and then rises slowly. [5]
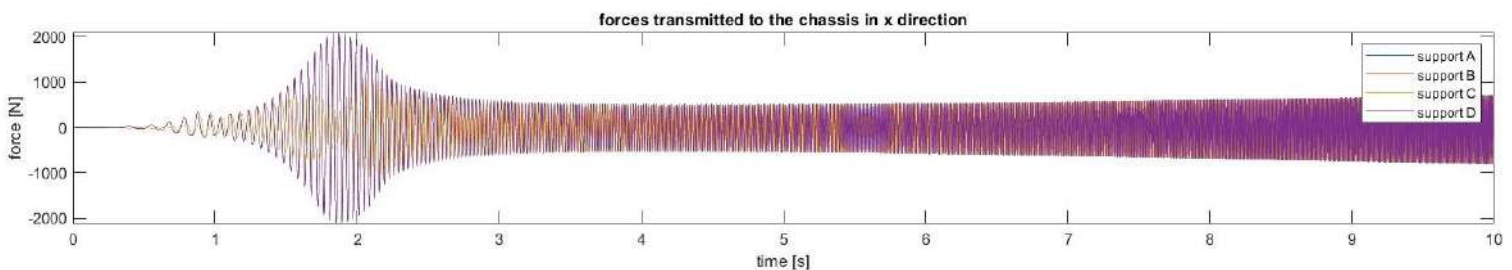

FIGURE 13: FORCES TRANSMITTED TO THE CHASSIS IN X DIRECTION

11

FEA AND MULTIBODY DYNAMICS VALIDATION

To validate the modal analysis results from the MATLAB script, a normal modes analysis has been performed by means of a multibody dynamics software MSC Adams [6]. The engine has been modeled as a rigid block, where the COG position, the mass and the inertia matrix has been defined from the data collected in the CAD model. Subsequently, every engine mount has been simulated by three linear springs, directed along the three-reference system axis. The normal modes analysis gave as a result the natural frequencies and the modal participation factors, which are scalars that measure the interaction between the modes and the directional excitation in a given reference frame. Larger values indicate a stronger contribution to the dynamic response.
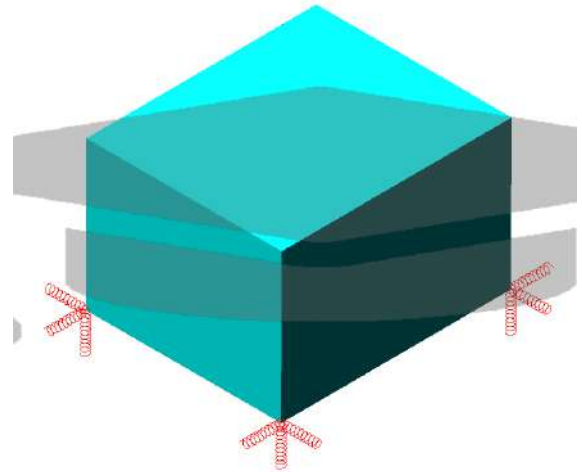

FIGURE 14: ADAMS MODEL

MODE NUMBER	NATURAL FREQUENCY	T1	T2	T3	R1	R2	R3
1	8.98262	0.0066746	1.28793e-18	7.38951e-09	3.0724e-06	2.009	1.97616
2	9.83144	6.55836e-09	3.06607e-18	0.0050882	1.27543	1.29079	1.17063e-06
3	13.5732	4.47121e-18	0.00257948	2.12941e-18	0.776424	1.32918e-14	0.655189
4	21.431	0.000491602	4.9621e-20	2.40902e-09	9.82914e-07	0.14803	0.142831
5	27.3253	4.31394e-08	2.99253e-19	1.90097e-05	0.0090408	0.126984	1.46096e-05
6	28.1739	3.33071e-09	1.21089e-18	0.000180123	0.0868184	0.0331548	1.14318e-06
Total		0.00716625	0.00257948	0.00528734	2.14771	3.60795	2.77419

FIGURE 15: MODAL PARTECIPATION FACTOR

To visualize the modal shapes and to validate the modal participation factors, a finite element modal analysis of the engine has also been performed. The mesh size ranges in between 1mm and 5mm, depending on the most critical dimension of the component considered. The material properties have been defined with the correct values of densities but also with infinite stiffness values, to obtain the correct inertia matrix and to satisfy the rigid body assumption. The engine components have been connected by contact surfaces, while the engine mounts have been modeled by 1D CBUSH elements. A property defining the stiffness value along the x, y and z direction has been assigned to every CBUSH element. [7]
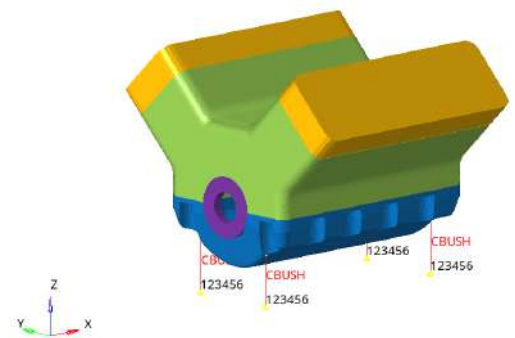

FIGURE 16: FEM MODEL

The natural frequency obtained from the MATLAB SCRIPT, the multibody dynamics software and the FEA are comparable, as figure 17 states. [8]

MODE	MATLAB [Hz]	FEA [Hz]	MSC ADAMS [Hz]	FEA DIFFERENCE [%]	ADAMS DIFFERENCE [%]
1	9.1964	9.148	8.98262	0.53	2.32
2	9.845	9.8638	9.83144	0.19	0.14
3	13.5732	13.765	13.5732	1.41	0.00
4	21.9917	21.7245	21.431	1.22	2.55
5	25.4063	25.76	27.3253	1.39	7.55
6	28.8034	28.9228	28.1739	0.41	2.19

FIGURE 17: NATURAL FREQUENCIES COMPARISON

From the FEA results, it has been possible to observe the mode shape of the engine, by means of a graphic post-processor. The results obtained are consistent with the modal participation factors values obtained from the multibody dynamic analysis and with the MATLAB modes plot.

CONCLUSION

This analysis is fundamental to analyze the vehicle NVH behavior, which is essential for achieving a pleasurable driving experience and enhancing the overall driver sensations.

The steady state analysis allows to better understand the vibration magnitude and trend when cruising at constant speed, while the ramp test is useful to analyze the vibration behavior when accelerating or decelerating.

As expected, the inertial forces magnitude is quite small due to the natural forces balancing of the 90-degree V6, while the moments intensity is significative.

Consequently, the displacements of the engine COG are negligible if compared to the rotations.

The natural frequency and the resonance frequency are close to each other due to the low damping ratio value chosen. The analysis of those frequencies is crucial, because if the engine is operated in such a way that the inertia forces and moments have the same frequencies, severe vibration amplitude take place, which can cause noise and failures.

The magnitude of the forces transmitted to the chassis exhibits the maximum values in the resonance frequency range, between 550 and 1800 rpm, and for frequencies near to it. After the resonance frequencies are crossed, the force amplitude is much lower. To improve the vehicle low-speed drivability, it's possible to reduce those forces in the low rpm range by adding countershafts and tuning the stiffness and damping values of the engine mounts.

The main problem found is that, when cruising on the highway at the speed legal limit in the top gear, the engine rotates at 2000 rpm, which is a critical regime: the forces transmitted to the chassis and the engine COG displacement exhibit great magnitude, mainly because the rotation frequency is in the resonance frequencies range. This needs to be solved like discussed previously or by tuning the top gear ratio to change the rotation speed frequency.

In a deeper analysis, it's possible to not adopt the rigid body hypothesis, to include the engine stiffness (and so its deformations) into the study.

REFERENCES

[1]   Maserati S.P.A.

[2]   Dassault Systems, *2023 SOLIDWORKS Student Edition.*

[3]   F. Pellicano, *Mechanical Vibration*, 2020 edition.

[4]   M. Callegari, P. Fanghella, F. Pellicano, *Meccanica applicata alle macchine*, CittàStudiEdizioni, 2017.

[5]   MathWorks, *MATLAB R2023b*

[6]   Hexagon AB, *MSC Adams Student Edition.*

[7]   Altair S.p.a., *Hyperworks 2023 suite Student Edition*

[8]   Microsoft Corporation, *Office 365 Excel*